AGU PUBLICATIONS

JGR

Journal of Geophysical Research: Solid Earth

RESEARCH ARTICLE
10.1002/2015JB012283

Key Points:
- The atomic attempt time and the magnetic grain size distribution are determined
- No consistent temperature dependence of the attempt time is found
- The attempt time is found to be strongly sample dependent

Correspondence to:
T. Berndt,
t.berndt13@imperial.ac.uk

Citation:
Berndt, T., A. R. Muxworthy, and G. A. Paterson (2015), Determining the magnetic attempt time τ_0, its temperature dependence, and the grain size distribution from magnetic viscosity measurements, *J. Geophys. Res. Solid Earth*, *120*, doi:10.1002/2015JB012283.

Received 15 JUN 2015
Accepted 25 OCT 2015
Accepted article online 28 OCT 2015

Determining the magnetic attempt time τ_0, its temperature dependence, and the grain size distribution from magnetic viscosity measurements

Thomas Berndt[1], Adrian R. Muxworthy[1], and Greig A. Paterson[2]

[1]Department of Earth Science and Engineering, Imperial College London, London, UK, [2]Key Laboratory of Earth and Planetary Physics, Institute of Geology and Geophysics, Chinese Academy of Sciences, Beijing, China

Abstract A new method to determine the atomic attempt time τ_0 of magnetic relaxation of fine particles, which is central to rock and soil magnetism and paleomagnetic recording theory, is presented, including the determination of its temperature dependence, and simultaneously the grain size distribution of a sample. It is based on measuring a series of zero-field magnetic viscous decay curves for saturation isothermal remanent magnetization at various different temperatures that are later joined together on a single grain size scale from which the grain size distribution and attempt time are determined. The attempt time was determined for three samples containing noninteracting, single-domain titanomagnetites of different grain sizes for temperatures between 27 K and 374 K. No clear temperature-dependent trend was found; however, values varied significantly from one sample to the other: from 10^{-11} to 10^{-8}s; in particular, the sample containing multiple magnetic phases had an effective attempt time significantly lower than the more homogeneous samples, thereby questioning the applicability of the simple Néel-Arhennius equation for magnetic relaxation for composite materials.

1. Introduction

The relaxation time τ of fine magnetic particles plays an important role in palaeomagnetic studies as it determines whether or not a remanent magnetization can be preserved over geological timescales. Grains that have a remanent magnetization that is kept by some energy barrier can be remagnetized because of thermal energy that causes random excitations to the grain's magnetization. The relaxation time is a measure of how long it takes, on average, for a grain to overcome its energy barrier by thermal excitations and become remagnetized. It is given by the Néel-Arhennius equation [*Néel*, 1949]

$$\frac{1}{\tau} = \frac{1}{\tau_0} \exp\left\{-\frac{\mu_0 H_K M_s V}{2kT}\right\}, \tag{1}$$

where μ_0 is the vacuum permeability, H_K is the microscopic coercivity, M_s is the spontaneous magnetization, V is the grain volume, k is the Boltzman constant, T is temperature, and τ_0^{-1} is a frequency factor that is known as the atomic attempt time. The attempt time is an average timescale between two successive random thermal excitations.

All the quantities in the equation are well known or can easily be determined, except τ_0, which is poorly constrained. *Néel* [1949] derived an expression to calculate τ_0 from fundamental material properties:

$$\frac{1}{\tau_0} = \frac{q_e \mu_0 H_K}{m_e} \left|3G\lambda + \mu_0 D M_s^2\right| \sqrt{\frac{2V}{\pi G k T}}, \tag{2}$$

where q_e and m_e are the charge and mass of an electron, respectively, G the shear modulus, λ is the longitudinal saturation magnetostriction, and D is a numerical coefficient which varies from $4\pi/5$ for a sphere to π for a cylinder. The first term in the addition represents the magnetoelastic energy and the second one the demagnetizing field. The latter one is significantly smaller than the first and can be neglected [*Néel*, 1949]. Based on slightly different assumptions, *Brown* [1959] derived a different expression, which nonetheless gives similar values. Both theories predict a temperature and volume dependence $\propto \sqrt{T/V}$, as well as an implicit dependence through the quantities that depend on temperature (H_K, G, and M_s).

Experimental studies tried to determine τ_0 for common magnetic minerals using a variety of methods, but due to the exponential nature of the dependence of τ_0 on the measurable quantities, it is difficult to determine it accurately; stated values in literature vary by several orders of magnitude, from 10^{-8} to 10^{-13}s [e.g., *Xiao et al.*, 1986; *Labarta et al.*, 1993; *Dickson et al.*, 1993; *Fabian*, 2006], with 10^{-9}s being the most commonly stated value. Moreover, τ_0 is generally assumed to be constant and any temperature and grain size dependence is usually neglected.

One approach to determine τ_0 is to measure the relaxation of magnetic particles at two different timescales t_1 and t_2 and correspondingly two different temperatures T_1 and T_2. If two (identical or different) experiments are designed that activate the same energy barriers $\mu_0 H_K M_s V$ (i.e., the same grains), then from equation (1) follows

$$\frac{T_1}{VH_K M_s} \ln \frac{t_1}{\tau_0} = \frac{T_2}{VH_K M_s} \ln \frac{t_2}{\tau_0}, \tag{3}$$

which can be solved for τ_0. *Dickson et al.* [1993] did this by using a combination of zero-field magnetic relaxation experiments and Mössbauer spectroscopy to measure τ_0 for iron oxyhydroxide particles in ferritin: The timescale for the magnetic decay in zero field is about 100 s and gives a blocking temperature of 9 K, while the timescale for the Mössbauer spectroscopy is 5×10^{-9}s and gives a blocking temperature of 36 K. This results in an attempt time of $\tau_0 = 1.1\times10^{-12}$s. *Moskowitz et al.* [1997] applied the same method to maghemite particles and obtained $T_B = 300$K for the Mössbauer spectroscopy and $T_B = 18$K for the magnetic measurements, which gives an attempt time of $\tau_0 = 1.1\times10^{-9}$s. These methods hence use just two data points to obtain τ_0, obtained by two different methods at very different temperatures, making it hard to quantify errors. *McNab et al.* [1968] used only Mössbauer spectra and fitted them to a model equation to obtain τ_0 for magnetite particles and obtained a value of 9.5×10^{-10}s.

Worm and Jackson [1999] measured the frequency dependence of susceptibility (FDS) at different temperatures of samples of the Tiva Canyon (containing noninteracting single-domain low-Ti titanomagnetite) to calculate the attempt time. They obtained $\tau_0 = 10^{-9}$s for most samples, except one that contained larger grains, for which they obtained $\tau_0 = 10^{-11}$s. Afterward, they gave the samples an isothermal remanent magnetization or a thermal remanent magnetization and thermally demagnetized them. From the demagnetization data they obtained the grain size distributions of the samples.

Shcherbakov and Fabian [2005] used the same FDS data to directly calculate the grain size distribution but found a significant misfit between the different temperature data. They note that the fit is improved by using $\tau_0 = 10^{-13}$s but consider this low value unphysical. Instead, they suggest that by taking magnetostatic interactions into account, the misfits can be eliminated and the τ_0 values obtained by *Worm and Jackson* [1999] remain valid. Moreover, *Shcherbakov and Fabian* [2005] found that their FDS approach tended to show more fine-grained particles than the distributions obtained by thermal demagnetization and suggested that this is because thermal demagnetizations tend to suppress viscous magnetizations.

Labarta et al. [1993] and *Iglesias et al.* [1996] used a different method. They measured various relaxation curves of thermoremanent magnetizations (TRM) at different temperatures. When plotting these curves versus the scaling variable

$$T \ln\left(t/\tau_0\right) \tag{4}$$

instead of time t, all the decay curves should match up at their ends to form a single "master curve" (terminology of the authors). They base this argument on the observation that time and temperature appear in the energy barrier equation for particles to change their magnetization and the remanent magnetization is an integral over the energy barriers

$$E = kT \ln\left(\frac{t}{\tau_0}\right). \tag{5}$$

The curves will, however, only match up for an appropriate choice of τ_0, thereby offering the possibility of finding the τ_0 that creates the best fit. While there method leads to reasonable estimates of τ_0 on the order of 10^{-13} to 10^{-7}, there are a number of unresolved issues:

1. The magnetization data had to be normalized, and the authors used "an arbitrary reference magnetization M_0." The choice of this normalization, however, has an effect on the best fit τ_0: In their magnetization versus $T \ln\left(t/\tau_0\right)$ plots, M_0 moves the pieces of the curve [see, e.g., *Labarta et al.*, 1993, Figure 5] vertically, while τ_0

moves them horizontally. Hence, there are many possible choices of (M_0, τ_0) to make the curves fall onto a single master curve.
2. The variation of M_s with temperature is not taken into account.
3. There is no mathematical criterion given of how to determine a best fit τ_0.

In this study, the same principle is used, but the mathematics are rigorously derived and an objective criterion of "the best fit" choice of τ_0 for the various decay curves is defined.

This is done by making use of the work of *Walton* [1980]. He started from the fact that an assembly of identical grains of a given volume V, the viscous acquisition/decay of their magnetization is given by

$$n - n_{\mathrm{eq}} = \left(n - n_{\mathrm{eq}}\right)_{t=0} e^{-t/\tau}, \tag{6}$$

where $n = n_+ - n_-$, the difference between the number n_+ of magnetic moments that are aligned with the applied field and the number n_- that are in the opposite direction, and n_{eq} is its equilibrium value that the assembly tends to after infinite time. He integrated this equation for assemblies of a grain volume distribution $f(V)$ to give

$$\frac{\partial M}{\partial \ln t} = \frac{\sqrt{2\pi}}{e}\left(n - n_{\mathrm{eq}}\right)_{t=0} f\left(\frac{kT}{K}\ln\frac{t}{\tau_0}\right)\left(\frac{kT}{K}\right)^2 \ln\left(\frac{t}{\tau_0}\right) M_s, \tag{7}$$

where e is Euler's number, and $K = \mu_0 H_K M_s/2$ is the magnetic anisotropy constant. In this paper, this equation is only integrated (over $d\ln t$) for the case of the magnetic acquisition in field of an initially demagnetized sample, for which $n_{t=0} = 0$ and $n_{\mathrm{eq},t=0} = M_s VH/3kT$, where H is the external field. It followed that the intensity of remanent magnetization M is given by

$$M(t) = \frac{BH}{3+r}\left(\frac{kT}{M_s^2}\right)^{2+r}\left(\ln\frac{t}{\tau_0}\right)^{3+r}, \tag{8}$$

where B is a constant. In equation (8), a grain volume distribution proportional to V^r has been assumed for simplicity; but this dependence approximates a lognormal distribution for the larger grains. *Walton* [1980] points out that the viscous behavior of a sample depends on the grain size distribution, that is, on the choice (or choices in the case of a power series) of r that best represents the distribution. As the scaling variable (4) by *Labarta et al.* [1993] does not appear in this expression, it is not an appropriate choice in this case.

2. Theory

2.1. Relating Magnetic Intensity to Blocking Volume

A much easier case that is not described in the paper by *Walton* [1980] is the magnetic decay of an initially fully magnetized sample. Such a state is easily created experimentally by applying a saturating isothermal remanent magnetization (SIRM). In this case, $n_{t=0} = n_0$, that is, a constant; the number of grains magnetized along the field direction at time $t = 0$ equals the total number of grains. Note that an SIRM produces exactly the same state regardless of the temperature at which the SIRM was acquired. If the decay of remanence is observed in zero field, then $n_{\mathrm{eq},t=0} = 0$, which further simplifies the mathematics. For single-domain grains, equation (7) is then easily integrated by substituting the blocking volume

$$V_B = \frac{2kT}{\mu_0 H_K M_s}\ln\frac{t}{\tau_0}, \tag{9}$$

which gives

$$\frac{\partial M}{\partial \ln t} = \frac{\partial M}{\partial V_B}\cdot\frac{\partial V_B}{\partial \ln t} = \frac{\sqrt{2\pi}}{e} n_0 f\left(V_B\right)\frac{2kT}{\mu_0 H_K M_s} V_B M_s.$$

Dividing by the time derivative gives

$$\frac{\partial M}{\partial V_B} = \frac{\sqrt{2\pi}}{e} n_0 f\left(V_B\right) V_B M_s.$$

Integrating over V_B, one obtains

$$M(t) = \frac{\sqrt{2\pi}}{e} n_0 M_s \int f\left(V_B\right) V_B \, dV_B \tag{10}$$

or

$$M(t) = \frac{\sqrt{2\pi}}{e} n_0 M_s F\left(V_B\right) , \tag{11}$$

where F is a function that depends on the grain size distribution and V_B. Contrary to equation (8), however, this relation does not explicitly depend on time, but there is a time dependence through V_B. If we normalize M by M_s (which is temperature dependent), we obtain

$$\tilde{M} = \frac{M}{M_s} \propto F\left(V_B\right) .$$

The normalized intensity $\tilde{M}$ therefore only depends on time and temperature through V_B. Hence, we can design an experiment where we induce an SIRM and measure $\tilde{M}$ as a function of time t at given a temperature T. If in two experimental runs at two different temperatures T_1 and T_2, we find that the normalized intensity $\tilde{M}$ is the same at time t_1 and t_2, respectively, then the blocking volume V_B must also be the same at these two times/temperatures: Hence, any given intensity $\tilde{M}$ corresponds to a given blocking volume V_B.

2.2. Calculating the Attempt Time τ_0

We derive an equation to calculate the attempt time τ_0 as a function of temperature and volume from the normalized intensity $\tilde{M}(T, t)$. To simplify the notation, we define $a = \sqrt{2\pi} e^{-1} n_0$ and $V = V_B$. Then equation (10) becomes

$$\tilde{M} = a \int f(V)\, V\, dV. \tag{12}$$

Assuming that shape anisotropy is dominant and therefore $H_K = NM_s$, we can define a new "temperature scale"

$$x = \frac{2kT}{\mu_0 M_s^2(T)}, \tag{13}$$

such that equation (9) becomes

$$V = \frac{x}{N}\left(\ln t - \ln \tau_0\right) . \tag{14}$$

Taking logarithmic time and x "temperature" derivatives of V, respectively, one obtains

$$\frac{\partial V}{\partial \ln t} = \frac{x}{N} \tag{15}$$

$$\frac{\partial V}{\partial \ln x} = \frac{x}{N}\left(\ln t - \ln \tau_0\right) . \tag{16}$$

Here we are neglecting the time and temperature derivatives of τ_0 itself, as τ_0 is expected to vary much less than the other quantities. Using the chain rule, the respective derivatives of the normalized magnetization are then

$$M_t \equiv \frac{\partial \tilde{M}}{\partial \ln t} = \frac{af(V)\, Vx}{N} \tag{17}$$

$$M_x \equiv \frac{\partial \tilde{M}}{\partial \ln x} = \frac{af(V)\, Vx}{N}\left(\ln t - \ln \tau_0\right) , \tag{18}$$

where the subscripts stand for the respective derivatives. Dividing, we get

$$\frac{M_x}{M_t} = \ln t - \ln \tau_0, \tag{19}$$

which is readily solved for the attempt time

$$\tau_0 = t \exp\left\{-\frac{M_x}{M_t}\right\} . \tag{20}$$

2.3. Calculating the Grain Size Distribution

Once the attempt time is known, it is easy to solve for the grain volume. From equations (13) to (14) follow

$$NV = \frac{kT}{\mu_0 M_s^2(T)} \ln \frac{t}{\tau_0}. \tag{21}$$

To solve explicitly for the volume, one would need to know the shape factor N, which can vary from 0 (for a perfect sphere) over 0.5 (for a needle-like particle) to 1 (for a plate). For a natural assemblage, we can therefore make a rough estimate of N, as any given grain formation process typically forms grains of similar shape (e.g., needle-like particles). The volume V, on the other hand, can span multiple orders of magnitude in a single sample and is therefore of greater interest to be calculated from the experimental data. The grain size distribution is obtained by taking the derivative of equation (12), which gives

$$\frac{\partial \tilde{M}}{\partial V} = af(V)V \tag{22}$$

and

$$n_0 f(V) = \frac{e}{\sqrt{2\pi V}} \frac{\partial \tilde{M}}{\partial V}. \tag{23}$$

The total number of (activated) grains and the total volume can be found by calculating the integral.

3. Samples and Methods

3.1. Samples

In order to test the theory, samples should ideally contain noninteracting, single-domain (SD) grains that were superparamagnetic at room temperature (or slightly above). The latter criterion permits to perform the experiments at low temperature, thereby avoiding problems with thermal alteration. Three samples from the Tiva Canyon Tuff that have previously been well characterized and described by *Jackson et al.* [2006], *Till et al.* [2011], and others [*Schlinger et al.*, 1988, 1991; *Rosenbaum*, 1993; *Worm and Jackson*, 1999; *Egli and Lowrie*, 2002; *Shcherbakov and Fabian*, 2005] fulfilled these criteria. These samples contain mostly noninteracting SD grains of slightly impure magnetite of narrow grain size distributions. The impurities are around 10% (TM10) and are mainly Ti, Mn, and Cr [*Jackson et al.*, 2006]. The three samples, TC04-12-01, TC04-11-M, and TC04-12-07 (12-01, 11-M, and 12-07, respectively), originate from three different layers of the Tiva Canyon. As described by *Till et al.* [2011], the grain size varies with stratigraphic height, from approximately 15 nm in length at the base of the Canyon to about 1000 nm at the top. Sample 12-01 is from one of the bottom layers, i.e., containing the smallest, and 12-07 is from a higher layer, i.e., containing the largest grains employed for this study. The samples were crushed into a powder and filled into plastic capsules for the experiments. Samples 12-01 and 12-07 came from single drilling cores, respectively, but sample 11-M was a mix of various cores from a single stratigraphic layer.

The grain sizes of various samples of the Tiva Canyon Tuff have been investigated by various different studies and methods and are summarized in Table 1. Among them are the direct observation by transmission electron microscopy by *Schlinger et al.* [1991], thermal demagnetization of an isothermal remanent magnetization (IRM) or TRM [*Worm and Jackson*, 1999], frequency-dependent susceptibility analysis [*Shcherbakov and Fabian*, 2005], and thermal fluctuation tomography [*Jackson et al.*, 2006]. While in this study, the samples 12-01 and 12-07 were taken from the bottom and top stratigraphic layer of the canyon, respectively, previous studies have only investigated the adjacent (second bottom and second top) stratigraphic layers. Nevertheless, given the trends in the stratigraphic sequence, a comparison with the adjacent layers 12-02 and 12-06 is informative (Table 1): Mean grain volumes as inferred by thermal fluctuation tomography are $1.4 \times 10^{-24}\mathrm{m}^3$ (sample 12-02) and $3.2 \times 10^{-24}\mathrm{m}^3$ (samples 11-M and 12-06), respectively, and width/length ratios of 0.24 (12-02), 0.22 (11-M), and 0.18 (12-06), respectively. These data translate to shape anisotropy demagnetizing factors of $\left(N_b - N_a\right) = 0.39$ (12-02), 0.40 (11-M), and 0.43 (12-06), respectively [*Stoner*, 1945].

Jackson et al. [2006] fitted temperature-dependent hysteresis loops to a model equation

$$M_s = M_{s,0}\left[\left(T_c - T\right) / \left(T_c - T_0\right)\right]^n \tag{24}$$

and obtained best fits for $n = 0.43$ and $T_c = 775$K, corresponding to TM12 titanomagnetite with a room temperature spontaneous magnetization of $M_{s,0} = 404$kA/m [*Hunt et al.*, 1995]. The fitting parameters a summarized in Table 2.

Table 1. Comparison of Grain Sizes Obtained by Different Methods[a]

		TEM			TRM/IRM/FDS		TFT				This Work	
Sample	Z	L	V	L/W	L	V	L	V	L/W	$N_b - N_a$	L	V
TC04-12-07	1.4										15–23	0.5–1.6
CS913	1.39	85	7.4	0.11								
TC04-12-06	1.1						46	3.2	0.18	0.43		
CS914	0.98	50	3.6	0.17	32	4	50	4.0	0.18			
TC04-11-M	0.75						40	3.2	0.22	0.40	$\ll 23$	$\ll 2.3$
CS915	0.57	37	2.0	0.2	22	1.8						
CS916	0.17	18	0.5	0.28	13	0.8						
TC04-12-02	0.12						29	1.4	0.24	0.39		
TC04-12-01	0.05										< 9	< 0.2
CS917	0.05	15	0.4	0.36			26	2.0	0.33			

[a] Z: stratigraphic height above the base of the flow, determined by measurements in the field; L: mean length of grains in nanometer; V: mean volume of grains in 10^{-24} m^3; $N_b - N_a$: shape demagnetizing factors calculated after *Stoner* [1945]. TEM: grain sizes determined by transmission electron microscopy by *Schlinger et al.* [1991]; TRM/IRM/FDS: determined by thermal demagnetization of IRM/TRM [*Worm and Jackson*, 1999] or FDS [*Shcherbakov and Fabian*, 2005], which gave nearly identical results; thermal fluctuation tomography (TFT) from *Jackson et al.* [2006]; this work: minimum grain sizes accessible by viscosity experiments of this work.

3.2. Equipment

Standard rock magnetic experiments (IRM acquisition curves, first-order reversal curves (FORC), and determination of Curie temperatures) were done on a Princeton Instruments vibrating sample magnetometer (VSM) at Imperial College London to extend the characterization of the samples done previously. The temperature-dependent viscosity and hysteresis experiments needed for the method have been carried out at the Institute of Rock Magnetism (all three samples, limited temperature ranges) of the University of Minnesota on a Quantum Design superconducting quantum interference device (SQUID) Magnetic Properties Measurement System 2 (MPMS2) and at the Diamond Light Source (a specimen of 12-07, over a broad temperature range) in Didcot, UK, on a VSM-MPMS.

3.3. Methodology

The method is based on two types of information: (1) spontaneous magnetization $M_s(T)$ and (2) viscous decay of remanence $M_r(T, t)$. To obtain this information, the experimental sequence has been designed as follows: (1) The sample is heated/cooled to a temperature T_i. (2) A partial hysteresis curve is measured from 0 T up to 2.5 T. (3) The field is switched off, and $M(t)$ is measured. (4) Then the sample is heated/cooled to the next temperature step T_{i+1}, and the process is repeated.

The second step provides the $M_s(T, H)$ data to calculate the spontaneous magnetization of the ferromagnetic material. As the hysteresis loop ends at 2.5 T, the sample is fully saturated at that point, and the field is quickly

Table 2. Summary of Hysteresis Loop Fitting Parameters and Comparison With Those of *Jackson et al.* [2006][a]

		TFT Fit		Hysteresis Loop Fit			Thermomagnetic Curves
Sample	Z	T_c	n	T_c	n	m	T_c
TC04-12-07 (MPMS2)	1.4			565	0.67	1.00	514
TC04-12-07 (VSM-MPMS)	1.4			579	0.69	1.13	514
TC04-12-06	1.1	502	0.43				
TC04-11-M	0.75	502	0.43	582	0.48	1.02	503 & 711
TC04-12-02	0.12	502	0.43				
TC04-12-01	0.05			580	0.47	1.10	471

[a] T_c: Curie temperature in Celsius; n and m fitting parameters of equation (25); Z: stratigraphic height in meter; TFT: thermal fluctuation tomography by *Jackson et al.* [2006].

(relatively speaking) switched off to measure the decay of a saturation isothermal remanent magnetization (SIRM). The decay has been measured for 20 min (1200 s, one specimen of 12-07, over a broad temperature range) or 3 h (10^4s, all samples) at each temperature step, taking approximately one data point every 14 s. Due to the fact that the instrument takes about a minute to reduce the field from 2.5 to 0 T, the data points for the first 200 s have been discarded. Hence, time scales of up to almost 2 orders of magnitude (2×10^2 s – 10^4 s) were measured.

3.4. Hystersis Loops and M_s

The raw data obtained in the experiment included various $M(t)$ curves for different temperatures and their corresponding partial hysteresis loops $M_s(H)$. It is imperative to have (1) very accurate M_s data that are corrected for any paramagnetic material and (2) very smooth $M(T,t)$ curves so one can calculate the derivatives.

To both smooth the M_s data and correct for the paramagnetic minerals, the raw $M_s(H,T)$ for fields >65% (above which the sample is considered to be fully saturated and field variation is due to paramagnetic materials) of the maximum field (which was 2.5 T) was fitted, using a least squares algorithm, to the model

$$M_s(H,T) = M_{s,0}\left(\frac{T_c - T}{T_c - T_0}\right)^n + C\left(\frac{H}{T}\right)^m, \tag{25}$$

where T_0 = 20°C is room temperature, $M_{s,0}$ is the spontaneous magnetization at room temperature, T_c is the Curie temperature, and C is the Curie constant of the paramagnetic material. The quantities $M_{s,0}$, T_c, n, m, and C are chosen such to obtain the best fit (the parameter m has been added to the Curie-Weiss law as it was found to give significantly improved fits). The filtered values of $M_s(H,T)$ are then obtained by using the fit values in equation (25), neglecting the paramagnetic term and setting $M_{s,0}$ equal to the theoretical value of the titanomagnetite composition of the sample, measured in units of magnetization (A/m), rather than in units of magnetic moment. The latter step is necessary as the instrument does not measure the magnetization but the magnetic moment, which in turn depends on the magnetic volume. Hence, there are three steps involved in the analysis of the hysteresis loops: first obtaining the raw $M_s(H,T)$ data, second fitting them to the model equation (25) ("fitted data"), and third neglecting the last term in the equation to obtain the corrected data (i.e., corrected for the paramagnetic minerals).

3.5. Magnetic Viscosity

Given the noise in the $M(T,t)$ data, it is impossible to calculate the derivatives M_x and M_t directly. Instead, a piecewise smoothing method similar to the one used for first-order reversal curves (FORC) has been employed: For each point (x,t) in temperature time space, a least squares plane fit was performed on the point and its nearest neighbors ±3 temperature steps and ±50 time steps (time steps were sampled on a logarithmic scale). The value of M at the center point $(\bar{x},\bar{t})$ that is the mean temperature and mean time (on a log-scale) of the fit was used for the smoothed value of $M(\bar{x},\bar{t})$ and the slopes in the x and t direction of the plane are used for the $M_x(\bar{x},\bar{t})$ and $M_t(\bar{x},\bar{t})$.

Moreover, the theory assumes an instantaneous decrease of the applied field H to zero, but the instruments need a finite time to reduce the field from 2.5 to 0 T. The time to change the field from 2.5 to 0 T was 112 s on the MPMS2 and 87 s on the VSM-MPMS, but as during some of this time the field is still large, we estimated an effective time for the first data point, based goodness-of-fit (97 s and 20 s, respectively, gave optimal fits). As this value is highly uncertain, the first few data points <200 s have been ignored in the analysis and as time appears only on a logarithmic scale in all the equations, the uncertainty of the timing of the first data point becomes negligible for longer time scales >200 s.

4. Results

4.1. Rock Magnetic Analysis

The FORCs (Figure 1) confirm a weakly interacting single-domain behavior for samples 12-01 and 12-07, but sample 11-M shows a more multidomain (MD)/interacting behavior. The thermomagnetic curves are shown in Figure 2. According to *Fabian et al.* [2013], in high fields the Curie temperature is best determined by finding inflection points (i.e., zeros of the second derivatives) of the $M_s(T)$ curves. Samples 12-01 and 12-07 are almost perfectly reversible and have Curie temperatures of around 471°C and 514°C, respectively, of the curves. In sample 11-M, the spontaneous magnetization is greatly reduced upon heating, and it has two magnetic phases: one with a Curie temperature around 503°C and another one with a Curie temperature around 711°C

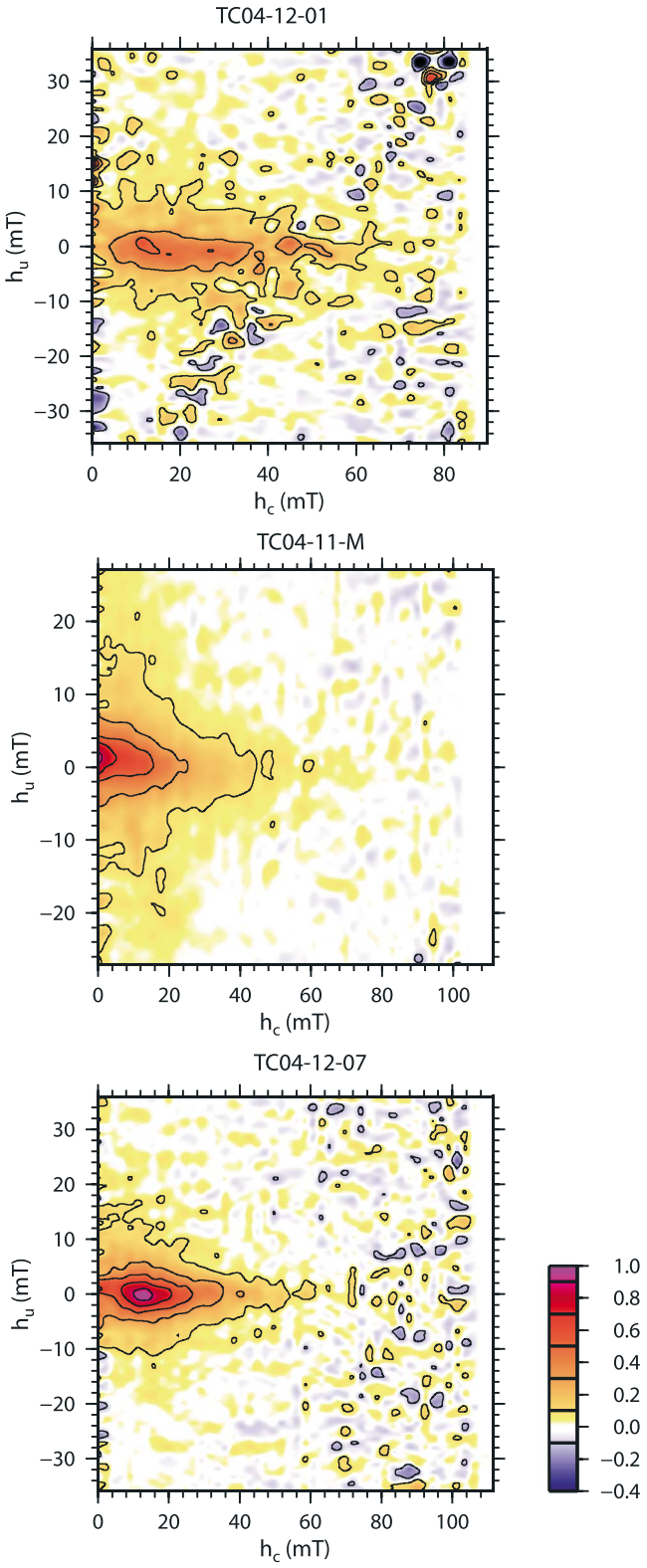

Figure 1. Room temperature FORCs of the three samples. Smoothing factor SF = 5; measuring time 300 ms per data point.

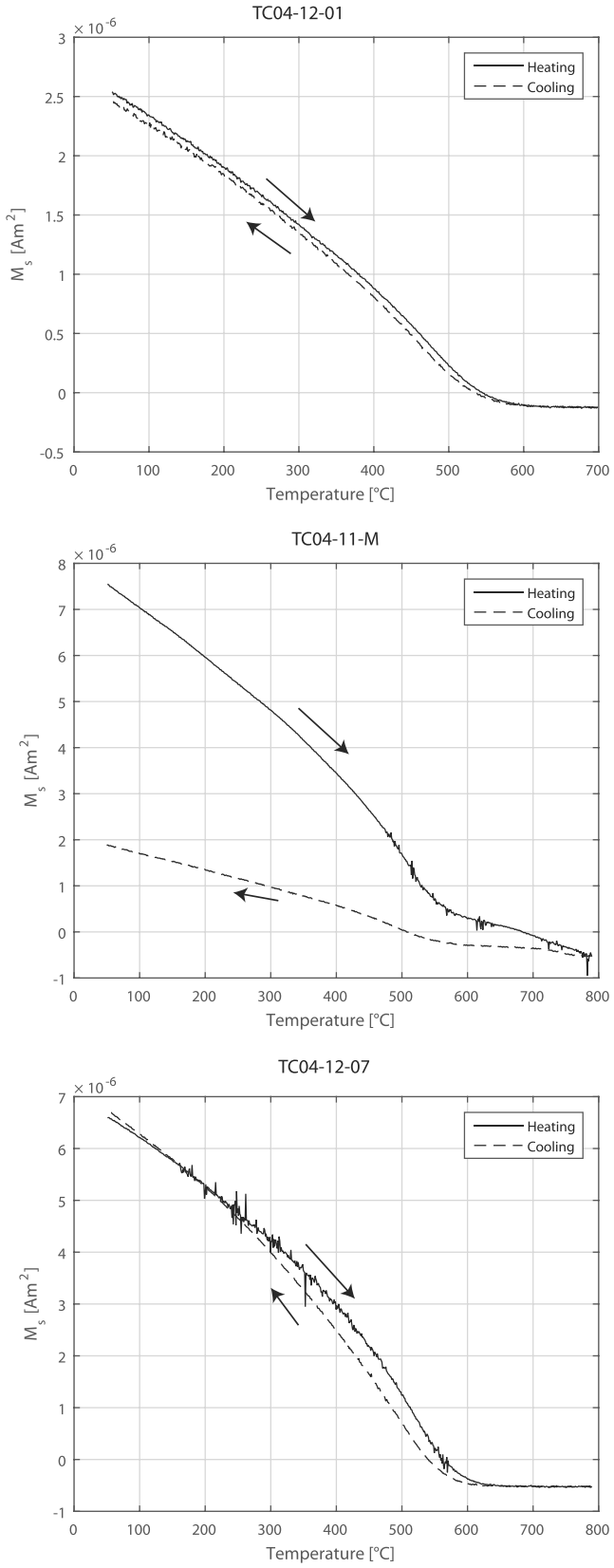

Figure 2. Thermomagnetic curves M_s (T) of the three samples in 1 T applied field.

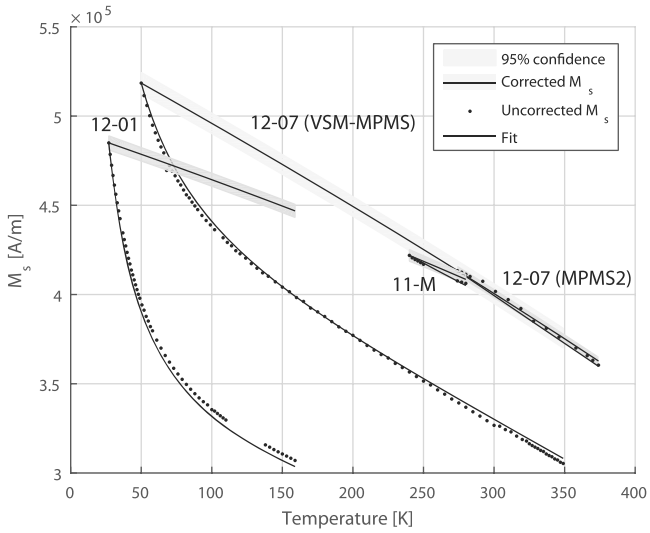

Figure 3. Spontaneous magnetization M_s (T) determined from hysteresis loops.

(using the traditional method of finding maxima of the second derivatives, the Curie temperatures would be slightly higher: 542°C for 12-01, 565°C for 12-07, and 552°C and 724°C for 11-M).

4.2. Hysteresis Loops and M_s

Figure 3 shows the results of the spontaneous magnetizations M_s as a function of temperature as determined from the hysteresis loops. The 95% confidence limits have been calculated. The M_s values are relatively well constrained for samples 12-01 and 12-07, but sample 11-M is poorly constrained; this is probably due 11-M having two different Curie temperatures (Figure 2). In order for the method to work, it is the slope of the M_s (T) curves that has to be determined very accurately, and not the absolute values of M_s. The best fit values are T_c=509°C, $n = 0.33$ for 12-01, T_c=610°C, $n = 0.45$ for 11-M, and T_c=559°C, $n = 0.67$ for 12-07. The Curie temperatures agree roughly with the values determined by the thermomagnetic analysis; though 11-M gives an intermediate value between the two Curie temperatures. It is, however, important to note that the aim of the fit is not to determine the Curie temperature but only to provide a way to smooth the M_s (T, H) data in a sensible way, and the matching Curie temperatures are merely a quality control.

Jackson et al. [2006] obtained $T_c = 502$°C and $n = 0.43$ for their Tiva Canyon samples. They used they equations by *Hunt et al.* [1995] to calculate the titanium content and the room temperature spontaneous magnetization $M_{s,0}$ of the samples from these values and obtained a TM12 composition with $M_{s,0} = 404$kA/m. We could apply the same equations to our experimental data, however, in order to better compare the results of the method by *Jackson et al.* [2006] and our method, we use the same value for $M_{s,0}$ they determined.

4.3. Magnetic Viscosity

Figure 4 shows the viscous decay plots of the three samples. The dotted lines are the raw measurements of the normalized magnetization versus time, while the continuous lines are the smoothed data as described in the previous section. In the magnification of sample 12-01 (Figure 4), it can be seen that around 100 K the lines of adjacent temperature steps start to overlap at about 2000 s, which is not a behavior that should be expected. The best explanation for this is a phase change, in particular a Verwey transition, which causes the magnetization of the different mineral phases to decay at different rates. In the calculation of the attempt time τ_0, outliers in this region have been removed.

The two plots of sample 12-07 in Figure 4 were measured on different instruments, a VSM-MPMS and a MPMS2, respectively. For the former, each temperature step was measured over a shorter time, which permitted measurements over the whole temperature range, where significant unblocking occurred. It can be seen that below 150 K and above 300 K, the slopes of the decay lines start to level off, meaning no significant unblocking occurs. In the MPMS2 this effect is less pronounced, as measurements were taken over longer timescales, leading to more unblocking at the same temperatures. Similarly, no significant unblocking occurs in sample 12-01 above 100 K. The limited unblocking in these temperature regions has important implications for the reliability of the τ_0 data.

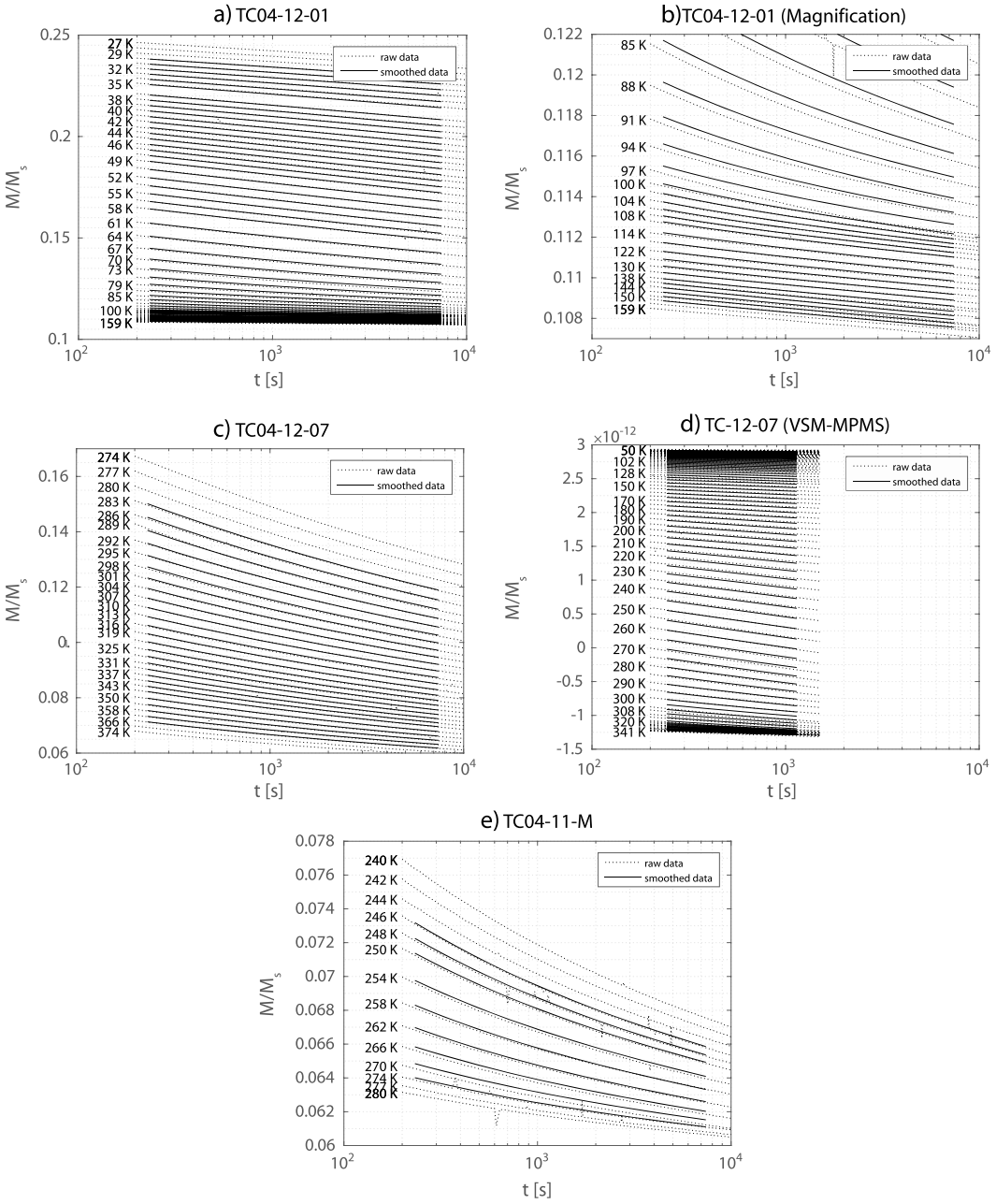

Figure 4. Plots of the viscous decay with time of the normalized magnetization after applying an SIRM at different temperatures.

5. Discussion

Using the data obtained from the hysteresis loops and the viscosity experiments, we can now test the theory and calculate the attempt time and the grain size distribution. When interpreting the results, one must, however, bear in mind the limitations of the accuracy of the viscosity data at temperatures with little unblocking.

5.1. Attempt Time τ_0

Figure 5 shows the calculated values of the attempt time τ_0 as a function of time and temperature. As can be seen, most variation occurs as a function of temperature rather than time. According to equation (2), τ_0 is expected to be both temperature and grain volume dependent. In theory, both of them can be inferred from the data in the plots, by using the definition of the blocking volume equation (9), which is a function of time

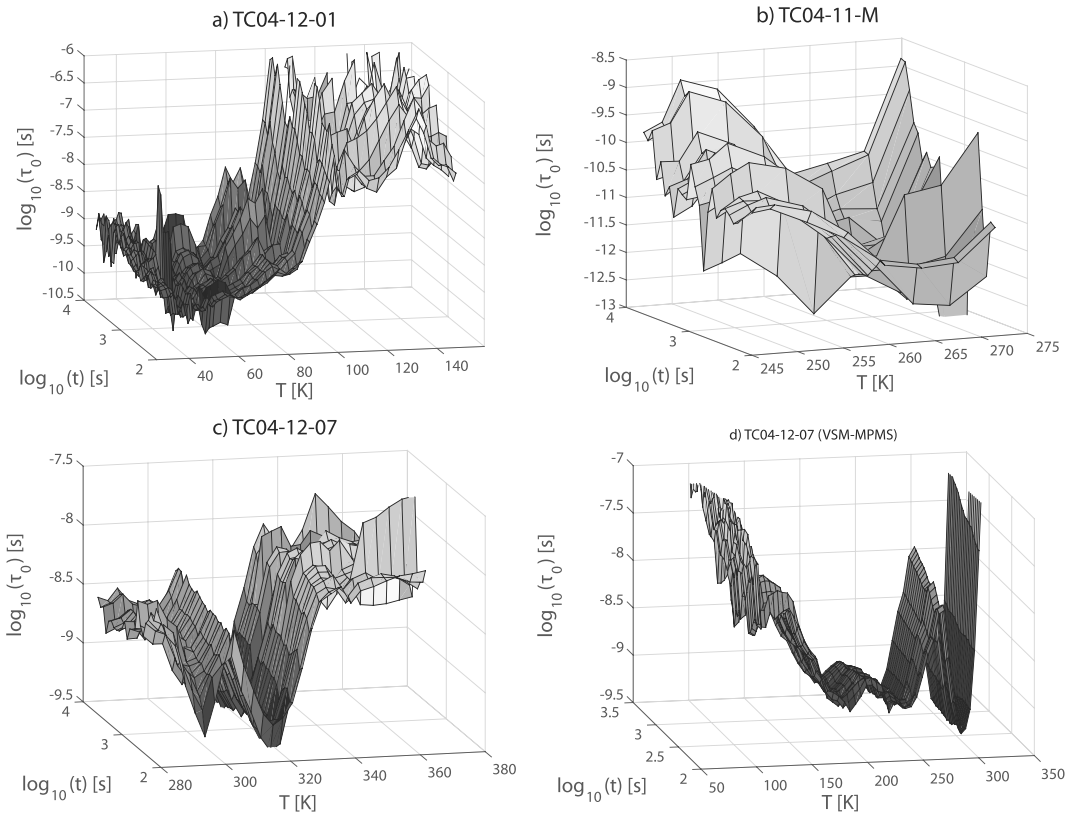

Figure 5. Calculated τ_0 values as a function of time and temperature.

and temperature. However, the focus of this study lies on the temperature dependence, mostly because in order to access a broad range of blocking volumes one needs to measure very long time scales. In this study however the maximum span of timescales on a logarithmic scale is from two to four (see Figure 5) and so no significant variation in τ_0 is expected. For this reason, the median attempt time has been calculated for each temperature step and plotted in Figure 6. Most obvious is the sharp increase in τ_0 to unrealistically high values in sample 12-01 around 100 K, and two sharp increases below 120 K and above 320 K in sample 12-07,

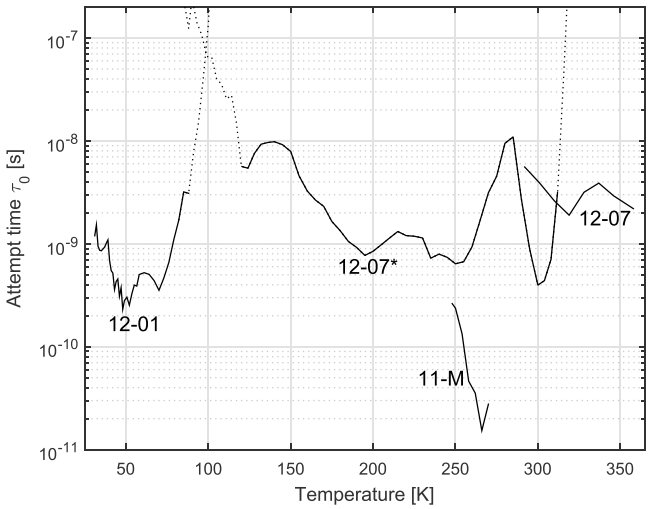

Figure 6. Median attempt time τ_0 versus temperature. Sample marked with a star was measured on a VSM-MPMS, the others on a SQUID-MPMS. Dotted lines indicate temperature ranges that are deemed unreliable because of insufficient unblocking.

Table 3. Summary of Median Values of τ_0[a]

Sample	Instrument	Temperature Range (K)	Timescale (s)	τ_0 (s)
12-01	MPMS2	27–159	10^4	6.6×10^{-10}
12-01	MPMS2	27–100	10^4	3.6×10^{-10}
11-M	MPMS2	240–280	10^4	1.7×10^{-11}
12-07	MPMS2	274–374	10^4	2.5×10^{-9}
12-07	VSM-MPMS	50–349	10^3	1.2×10^{-8}
12-07	VSM-MPMS	150–300	10^3	1.3×10^{-9}

[a]Narrower temperature ranges have been calculated in order to exclude unreliable data points.

when measured on the VSM-MPMS. The same sample measured over longer timescales in the MPMS2 does not show such a sharp increase. The temperature range at which two of these jumps occur suggest that, if this effect is real, it could be linked to the Verwey transition (through its effect on H_K that equation (2) depends on). There are, however, a number of reasons against this hypothesis: First, for sample 12-01, the attempt time increases, while for sample 12-07 the attempt time decreases. Second, the attempt time reaches values that are unphysically high. Third, only two out of three of these jumps occur close to the Verwey transition. Finally, these jumps consistently occur at temperatures where very little viscous decay (Figure 4) takes place. This means that the error in the time derivative of M_t may be large, and therefore, these results cannot be considered reliable. These regions are plotted as dotted lines in the figure. This also explains why this increase does not occur when sample 12-07 was measured over longer timescales on the MPMS2, as this means that more unblocking takes place at the same temperatures. Hence, we conclude that our method only works reliably at temperatures where significant decay takes place and that dotted areas in Figure 5 are artifacts due to experimental errors. Sample 11-M shows the lowest values of τ_0. This sample differed from the other two samples in that it was a mixture of powders of different cores from one layer in the Tiva Canyon and in that it showed a more MD/interacting behavior in the FORC (Figure 1).

Predicted from theory, equation (2) is a $\sqrt{T}$ dependence. This dependence cannot be confirmed with the data obtained in this study, however. Although τ_0 varies with temperature, there is no consistent trend. Therefore, median τ_0 was calculated for the whole temperature range, excluding the data that are deemed unreliable

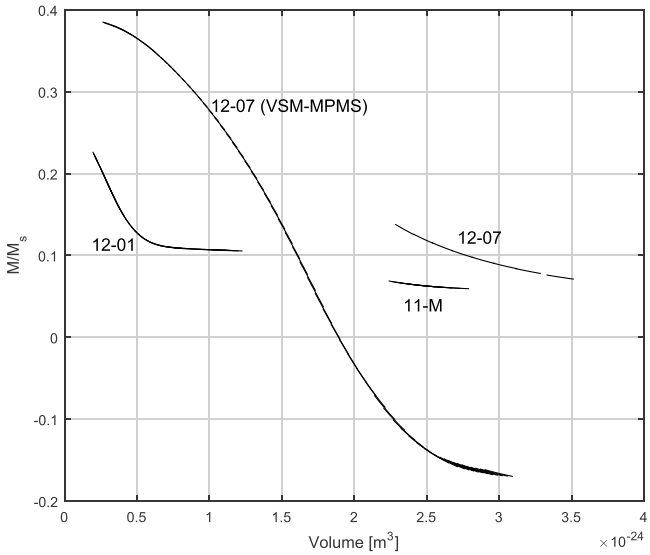

Figure 7. Viscous decay of the normalized magnetization versus grain size assuming anisotropy factors given in Table 1. The *y* axis shows the volume of the grains that are activated at any given temperature and time, given by equation (9); *x* axis shows the normalized magnetization M_r/M_s that is left after demagnetizing grains up to the given volume. The figure is created by plotting all decay plots from Figure 4 on a grain volume rather than a temperature or timescale—using the right attempt time τ_0 all the plots match up and fall onto a single curve.

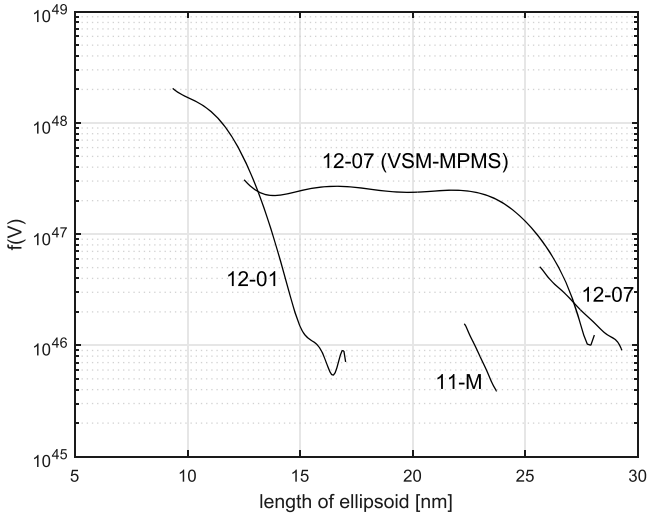

Figure 8. Grain size distributions using the median τ_0 for each sample assuming anisotropy factors given in Table 1.

(Table 3). It is, however, possible that there are real temperature variations of τ_0, that can, in principle, be found with the method outlined in this work, be doing more experiments with more samples, and most importantly, at longer timescales to increase the reliability of data points at temperatures of little unblocking.

5.2. Grain Size Distribution

The grain sizes of the grains that are demagnetized are calculated using equation (14) and assuming the anisotropy factors $(N_b - N_a)$ given in Table 1, as inferred from *Jackson et al.* [2006]. For each sample, the median attempt time $\bar{\tau}_0$ has been calculated and used to calculate the grain sizes. Figure 7 shows the decay of magnetization versus the grain size activated. The figure is created by using all the temperature steps in Figure 4, and converting their time axis to a volume axis using equation (14). This is similar to the "$T \ln(t/\tau_0)$-scaling" plots of *Labarta et al.* [1993] but takes the temperature dependence of M_s into account. In theory, all the lines should match up exactly. Figure 8 shows the grain size distributions of the three samples as calculated by equation (23).

By integrating the area under the plots, the total number of grains and the total volume of the grains activated can be obtained. These are $N_{tot} = 4.7 \times 10^{12}$, $V_{tot} = 1.3 \times 10^{-11}\text{m}^3$ for 12-07 (specimen used on the MPMS2 at high temperatures) and $N_{tot} = 3.6 \times 10^{12}$, $V_{tot} = 4.6 \times 10^{-11}\text{m}^3$ (specimen used on the VSM-MPMS at low and high temperatures), $N_{tot} = 9.1 \times 10^{11}$, $V_{tot} = 2.3 \times 10^{-12}\text{m}^3$ for 11-M and $N_{tot} = 4.1 \times 10^{13}$, $V_{tot} = 1.4 \times 10^{-11}\text{m}^3$ for 12-01.

Due to time constraints, the temperature spans of the experiments done on the SQUID-MPMS are not sufficient to cover the whole grain size distribution for any of the samples. It can be seen that in all samples, the most frequent grain size is smaller than the covered by the data. However, for sample 12-01, the grain size distribution is starting to level off on the left of the graph (Figure 8), and it can be assumed that the most frequent grain size is not much smaller than the smallest measured size of about 9 nm length. A specimen of sample 12-07 was remeasured on a VSM-MPMS over the whole temperature range available on the instrument and the number of grains is highest between 15 and 23 nm length. Table 1 summarizes the grain sizes obtained and compares them other studies of the Tiva Canyon samples that determined the grain sizes. Compared to the grain sizes obtained by other methods (transmission electron microscopy [*Schlinger et al.*, 1991], thermal demagnetization of IRM/TRM [*Worm and Jackson*, 1999], frequency-dependent susceptibility [*Shcherbakov and Fabian*, 2005], and thermal fluctuation tomography [*Jackson et al.*, 2006]), the viscous decay method consistently gives significantly smaller grain volumes.

6. Conclusions

The method described in this paper offers a new simple way to determine the attempt time τ_0 on a single instrument. It is an improvement over similar methods like the "$T \ln(t/\tau_0)$-scaling" [*Labarta et al.*, 1993] because it is mathematically rigorous and takes the temperature dependence of M_s into account. It was

successfully applied to three samples of weakly interacting single-domain titanomagnetite. It is found that τ_0 is strongly sample dependent, which is probably related to different unblocking spectra temperatures. Nevertheless, values of the order of 10^{-9} to 10^{-11} s are found. A single τ_0 estimate can be obtained in only 1 to 2 h by measuring only two or a few (for better statistics) adjacent temperature steps. In this case the method is simpler, faster, and avoids problems that might arise due to the use of two different experimental methods at widely different temperatures used in works such as those by *Dickson et al.* [1993] and *Moskowitz et al.* [1997]. Our proposed method, however, was found not to be reliable at temperatures where little unblocking takes place over the timescales used. Although the method can be used to create full grain size spectra, grain sizes tend to be underestimated when compared with other methods. Further development should therefore focus determining the grain size more accurately, the behavior of magnetic decay at temperatures that corresponds to little unblocking, and on the behavior of interacting, multidomain, and multimineral samples.

Acknowledgments
All experimental data are available upon request from the authors. The experiments at the Institute of Rock Magnetism were funded by an IRM Visiting Research Fellowship which is funded by the National Science Foundation, W. M. Keck Foundation, and the University of Minnesota. Many thanks to Paul Southern for providing the equipment and helping with preliminary experiments that lead to the development our method, to Mike Jackson for providing the Tiva Canyon samples, and to Alexey Dobrynin for giving us access to the high temperature MPMS-VSM.

References

Brown, W. F. (1959), Relaxational behavior of fine magnetic particles, *J. Appl. Phys.*, *30*, S130–S132, doi:10.1063/1.2185851.
Dickson, D., N. Reid, and C. Hunt (1993), Determination of f_0 for fine magnetic particles, *J. Magn. Magn. Mater.*, *125*, 345–350.
Egli, R., and W. Lowrie (2002), Anhysteretic remanent magnetization of fine magnetic particles, *J. Geophys. Res.*, *107*(B10), 2209, doi:10.1029/2001JB000671.
Fabian, K. (2006), Approach to saturation analysis of hysteresis measurements in rock magnetism and evidence for stress dominated magnetic anisotropy in young mid-ocean ridge basalt, *Phys. Earth Planet. Inter.*, *154*, 299–307, doi:10.1016/j.pepi.2005.06.016.
Fabian, K., V. P. Shcherbakov, and S. A. McEnroe (2013), Measuring the Curie temperature, *Geochem. Geophys. Geosyst.*, *14*, 947–961, doi:10.1029/2012GC004440.
Hunt, C. P., B. M. Moskowitz, and S. K. Banerjee (1995), Magnetic properties of rocks and minerals, in *Rock Physics and Phase Relations: A Handbook of Physical Constants*, vol. 97, edited by T. J. Ahrens, pp. 189–204, AGU, Washington, D. C.
Iglesias, O., F. Badia, A. Labarta, and L. Balcells (1996), Energy barrier distributions in magnetic systems from the Tln(t/τ0) scaling, *Z. Phys. B: Condens. Matter*, *100*(2), 173–178, doi:10.1007/s002570050108.
Jackson, M., B. Carter-Stiglitz, R. Egli, and P. Solheid (2006), Characterizing the superparamagnetic grain distribution $f(V, H_k)$ by thermal fluctuation tomography, *J. Geophys. Res.*, *111*, B12S07, doi:10.1029/2006JB004514.
Labarta, A., O. Iglesias, L. Balcells, and F. Badia (1993), Magnetic relaxation in small-particle systems: ln (t/τ 0) scaling, *Phys. Rev. B*, *48*(14), 10,240–10,246, doi:10.1103/PhysRevB.48.10240.
McNab, T. K., R. A. Fox, and A. J. F. Boyle (1968), Some magnetic properties of magnetite (Fe3O4) microcrystals, *J. Appl. Phys.*, *39*(12), 5703, doi:10.1063/1.1656035.
Moskowitz, B. M., R. B. Frankel, S. A. Walton, D. P. Dickson, K. Wong, T. Douglas, and S. Mann (1997), Determination of the preexponential frequency factor for superparamagnetic maghemite particles in magnetoferritin, *J. Geophys. Res.*, *102*(97), 671–680.
Néel, L. (1949), Théorie du trainage magnétique des ferromagnétiques en grains fins avec application aux terres cuites, *Ann. Geophys.*, *5*(2), 99–136.
Rosenbaum, J. (1993), Magnetic grain-size variations through an ash flow sheet: Influence on magnetic properties and implications for cooling history, *J. Geophys. Res.*, *98*(B7), 11,715–11,727.
Schlinger, C. M., J. G. Rosenbaum, and D. R. Veblen (1988), Fe-oxide microcrystals in welded tuff from southern Nevada: Origin of remanence carriers by precipitation in volcanic glass, *Geology*, *16*, 556–559.
Schlinger, C. M., D. R. Veblen, and J. G. Rosenbaum (1991), Magnetism and magnetic mineralogy of ash flow tuffs from Yucca Mountain, Nevada, *J. Geophys. Res.*, *96*(B4), 6035–6052.
Shcherbakov, V. P., and K. Fabian (2005), On the determination of magnetic grain-size distributions of superparamagnetic particle ensembles using the frequency dependence of susceptibility at different temperatures, *Geophys. J. Int.*, *162*, 736–746, doi:10.1111/j.1365-246X.2005.02603.x.
Stoner, E. C. (1945), The demagnetizing factors for ellipsoids, *Philos. Mag. Ser.*, *7*(36), 803–821, doi:10.1080/14786444508521510.
Till, J., M. Jackson, J. Rosenbaum, and P. Solheid (2011), Magnetic properties in an ash flow tuff with continuous grain size variation: A natural reference for magnetic particle granulometry, *Geochem. Geophys. Geosyst.*, *12*, Q07Z26, doi:10.1029/2011GC003648.
Walton, D. (1980), Time-temperature relations in the magnetization of assemblies of single domain grains, *Nature*, *286*(5770), 245–247, doi:10.1038/286245a0.
Worm, H.-U., and M. Jackson (1999), The superparamagnetism of Yucca Mountain tuff, *J. Geophys. Res.*, *104*, 25,415–25,426, doi:10.1029/1999JB900285.
Xiao, G., S. Liou, A. Levy, J. Taylor, and C. Chien (1986), Magnetic relaxation in Fe-(SiO_2) granular films, *Phys. Rev. B*, *34*(11), 7573.